We are IntechOpen, the world's leading publisher of Open Access books Built by scientists, for scientists

4,800
Open access books available

122,000
International authors and editors

135M
Downloads

Our authors are among the

154
Countries delivered to

TOP 1%
most cited scientists

12.2%
Contributors from top 500 universities

CLARIVATE ANALYTICS BOOK CITATION INDEX INDEXED

WEB OF SCIENCE™

Selection of our books indexed in the Book Citation Index in Web of Science™ Core Collection (BKCI)

Interested in publishing with us?
Contact book.department@intechopen.com

Numbers displayed above are based on latest data collected.
For more information visit www.intechopen.com

15

NIR Single Photon Detectors with Up-conversion Technology and its Applications in Quantum Communication Systems

Lijun Ma, Oliver Slattery, and Xiao Tang
Information Technology laboratory, National Institute of Standards and Technology
United States of America

1. Introduction

The performance of any quantum communication system is limited by its transmission loss and detection efficiency, both of which must be balanced for optimal overall system performance. For current fiber-optic based systems, the transmission loss is small in the near infrared (NIR) range, and many fiber-based communication systems and devices tend to use this wavelength range. Therefore, the 1310 nm and 1550 nm bands, both of which are in the NIR range, have become mainstream in the telecom industry. However, the most efficient and low cost single photon detectors, such as silicon based avalanche photodiodes (APD), do not work in the NIR wavelength range. Bridging this gap is, of course, essential for an optimal quantum communication system.

In current systems, the preferred types of single photon detectors include photocathodebased detectors, APD-based detectors and superconducting-based detectors. Photocathodebased detectors use an InGaAs/InP photomultiplier tube (PMT) or an InGaAs Microchannel plate (MCP) for single photon detection in the NIR range. APD-based detectors, on the other hand, may only use InGaAs/InP APDs when detecting NIR single photons. Almost all superconducting-based detectors work in the NIR and can be described by two main types, including the Transition Edge Sensor (TES) and Superconducting Single-Photon Detectors (SSPD). In addition to these mainstream detectors, single photon detection at NIR can be achieved using a technique known as frequency up-conversion. We discuss this alternative technique in detail in this chapter.

1.1 Single photon detectors

PMTs, first invented in the 1930's, are used in many scientific applications, especially in those that require very large photosensitive areas. The wavelength sensitivity of PMTs is determined by an electron multiplying coating on the photocathode. While many suitable materials are available for visible light and UV-sensitive photocathodes, NIR sensitivity is not easily attainable. Currently, only InGaAs/InP based PMTs can operate in the NIR range, and its performance is limited by very low quantum efficiency (QE) (1 % at 1600 nm) and large timing jitter (1.5 ns) [Hamamatsu, 2005]. MCPs are micro-capillary electron multipliers coated with an electron-emissive material and multiply photon-excited electrons from a photon cathode [Wiza, 1979]. MCPs usually have faster rise times and lower timing jitter

Source: Advances in Lasers and Electro Optics, Book edited by: Nelson Costa and Adolfo Cartaxo,
ISBN 978-953-307-088-9, pp. 838, April 2010, INTECH, Croatia, downloaded from SCIYO.COM

than is achievable with PMTs. However, similar to PMTs, MCPs are most suitable for the visible light range, and only InGaAs MCPs can work in the NIR range. These MCPs, like PMTs, are limited by low QE (~1 %) [Martin, J. & Hink P. 2003].

APDs, initially studied in the 1960s [Goetzberger et al, 1963], are the solid-state counterpart of PMTs. In an APD, a photon is absorbed in a bulk semiconductor, where it generates an electron-hole pair. With a sufficiently high electric field, carriers are accelerated to speeds where they can generate more electron-hole pairs though impact ionization, resulting in an avalanche multiplication. The silicone based APDs (Si-APD) are the most practical and widely used single photon detectors in recent years. Si-APDs have high QE with low noise levels in the visible light range and can work at room temperature. However, its QE decreases rapidly at wavelengths approaching NIR (i.e. longer than 1000 nm) and it does not work at the two telecom bands (1310 nm and 1550 nm). InGaAs/InP based APDs do work in NIR but with significant limitations. The ionization coefficient for electrons and holes in InGaAs are comparable, which leads to higher dark counts, a measure of the noise level in the detector [Lacaita et al., 1996]. To reduce this noise, the APD should be operated at very low temperatures. However, the cut-off wavelength of InGaAs shortens as the temperature decreases and the device loses sensitivity to 1550 nm photons at around -100 °C. Furthermore, trapped carriers in the device cause severe afterpulsing in this type of APD, especially at lower temperatures as the trapping lifetime becomes longer. Therefore, the operating temperature for this type of APD is set between -100 °C and -20 °C where the total dark count rate (combining those due to thermal generation and those due to afterpulsing) remains low and sensitivity to the desired wavelengths still exists. To overcome the severe influence of afterpulsing, commercial single photon counting modules based on InGaAs/InP APDs use active quenching and gated, or Geiger, mode operation to suppress the noise. However, with the gated rate limited to the MHz range, this does not satisfy the requirement of high-speed quantum communications. Recently, a self-difference technique has been developed for InGaAs APDs that suppresses the afterpulsing noise, and it has been successfully applied to a GHz quantum communication system [Yuan et al., 2007]. The InGaAs APD has about 10 % detection efficiency, but also about a 6 % afterpulse probability which contributes extra errors to the quantum communication system.

For some time now, superconducting technology has been used to implement single photon detectors in the NIR [Gol'tsman et al., 2001; Korneev et al., 2004; Hadfield et al., 2007; Takesue et al., 2007; Lita et al., 2008; Ma et al., 2009]. These types of detectors can have extremely low dark count rates and flat wavelength sensitivity extending far into theinfrared (IR) range. A TES, or TES microcalorimeter, consists of a piece of wolfram film, which is cooled below 100 mK. The film is kept at the transition edge of superconducting to normal conduction by Joule heating provided by the current from an associated circuit. In the TES detector, a photon is absorbed in the film producing a photoelectron which heats the electron system, raising its resistance and causing a drop in the current. TES detectors have no intrinsic limitation on QE, and currently achieve almost 100 % QE at the 1550 nm wavelength. However, the timing jitter of a TES detector is quite large (~ 100 ns), and therefore it is not suitable for high speed quantum communication systems. SSPD, or SNSPD (superconducting nanowire single-photon detectors), consists of a thin superconducting nanowire, which is meandered into a certain pattern. The detector is cooled to about 3 ^{o}K while the current in the nanowire is biased slightly lower than the critical current. When a photon is absorbed into the detection area, it will generate a hot

spot. The current is forced to flow though a smaller cross-section of the nanowire around the hot spot, causing the current density to exceed the critical current density, which results in the loss of superconducting. After a few picoseconds, the hotspot disappears and the detector is restored to the original sate. SSPDs have the advantages of very small timing jitter and a high counting rate in excess of a gigahertz. It also works in free-running mode, which is preferred for the optimal performance of a quantum communication system. However, because it must operate at very low temperatures, the bulky and costly SSPD systems become a considerable impediment for practical applications.

1.2 Up-conversion detectors

A single photon detector using frequency up-conversion technology, also simply called an up-conversion detector, is not a direct detection method. It uses a non-linear optical media to up-convert the frequency of photons in the NIR range to a shorter wavelength by a process known as sum frequency generation (SFG). The emerging photons, at visible wavelengths, are then detected using visible region single photon detectors. Single photon detectors at the visible light region, such as the Si-APD, typically have high efficiency, low noise, can be operated in ambient temperatures, and are compact, inexpensive and practical. While up-conversion technology for strong light is not new [Midwinter & Warner 1967; Gurski, 1973], the up-conversion for single photon levels of light was achieved at the beginning of this century [Kim et al., 2001], and highly efficient up-conversion at single photon levels has only recently been demonstrated by using bulk periodically poled lithium niobate (PPLN) crystals [Vandevender & Kwiat, 2004] or PPLN waveguides [Xu et al., 2007; Diamanti et al., 2005; Langrock et al., 2005; Thew et al., 2006; Tanzilli et al., 2005]. Upconversion detectors work at room temperature, though the non-linear media is usually heated to satisfy a phase matching condition, described later, that is required for optimal conversion within the waveguide. The internal conversion efficiency of the waveguide can reach as high as 100 %, and the total QE for this type of detector is about 20 % ~ 35 %. The frequency up-conversion process does not contribute any significant timing jitter to the system. Instead, the timing jitter for this type of detector is influenced mainly by the Si-APD, and is usually in the region of 40 ps ~ 100 ps. Furthermore, the frequency up-conversion process provides some unique characteristics to the detector, such as narrow-band wavelength acceptance and polarization sensitivity, both of which are very useful for fiberbased quantum systems. To date, several groups have successfully developed highly efficient up-conversion detectors for the NIR range and have employed them in high speed quantum communications systems.

Table 1 summarizes the performance and characteristics of the various single photon detectors in the NIR range and an up-conversion detector, including their working temperature, maximum count rate, QE, dark count rate (DCR) and timing jitter.

In this chapter, we offer a general overview of the theoretical principles and experimental results of single photon detectors using frequency up-conversion technology, and its applications in quantum information systems. We begin with a brief introduction of nonlinear optics and its phenomena, especially the sum frequency generation in a quasi-phase matching (QPM) grating that is the basis of up-conversion technology. We then describe an up-conversion single-photon detector developed at the National Institute of Standards and Technology (NIST), and some key techniques used to implement the detectors with high efficiency, low noise, and low dark count rate. Finally, we introduce an existing quantum information, or quantum key distribution, system using up-conversion detectors.

Single photon detectors	Temperature, ° K	Maximum Count rate, Hz	QE, %	DCR, Hz	Timing jitter, ps
PMT (Hamamatsu)	193	10^7	1	160k	1500
MCP (Burle)	210	$1x10^6$	1	100k	1000
InGaAs APD (id Quantique)	Peltier cooled	$4×10^6$ (gated)	10	10 k	60
InGaAs APD (Toshiba, UK)	243	$4×10^8$	10	10 k	60
SSPD (NIST)	<3	10^9	1	10	60
TES (NIST)	<0.1	10^5	95	400	100000
Up-conversion detector (NIST)	Room*	$5×10^6$	31	2.5 k	100

Table 1. Performance of single photon detectors responsive in the NIR range. The data are from [Hamamatsu, 2005; Martin & Hink 2003, Ma et al., 2009; Takesue et al., 2007; Yuan et al., 2007; Xu et al., 2007; Lita et al. 2008].
* Although the up-conversion system itself is operated at room temperature, the non-linear crystal is heated locally to satisfy the phase matching condition required for optimal conversion.

2. Frequency up-conversion

2.1 Sum frequency generation

Frequency up-conversion technology is based on a second-order non-linear sum frequency generation process, in which two input photons (a signal and a pump photon) at different frequencies annihilate and another photon at their sum frequency is simultaneously generated in a second-order non-linear media as shown in Fig. 1(a). According to non-linear optics theory, this process can happen only if the following two conditions are satisfied:

$$\omega_s + \omega_p = \omega_o \tag{1a}$$

$$\vec{k}_s + \vec{k}_p = \vec{k}_o \tag{1b}$$

where ω_s, ω_p and ω_o are the angular frequencies of the signal, pump and the output light, respectively. $\vec{k}_s$, $\vec{k}_p$ and $\vec{k}_o$ are the wave vectors of the signal, pump and the output light. Eq. 1(a) specifies conservation of energy and Eq. 1(b) specifies conservation of momentum. The frequency sum generation process is illustrated in Fig. 1.

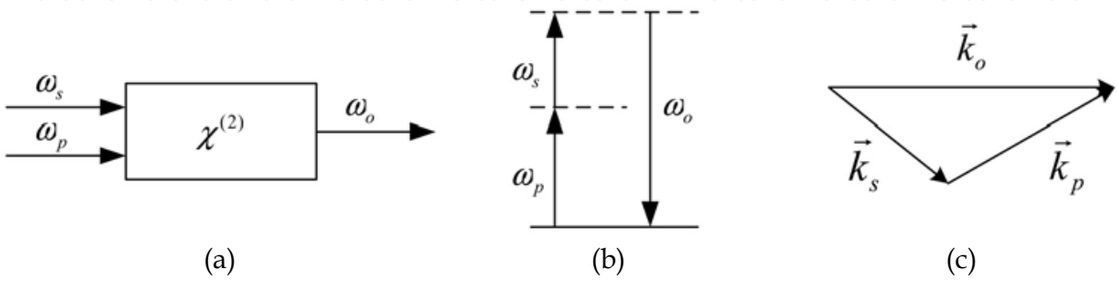

(a) (b) (c)

Fig. 1. Frequency up-conversion. (a) Geometry of the interaction. (b) Energy conservation condition. (c) Momentum conservation condition.

The nonlinear field evolution of the SFG process in a non-linear optical media can be described by:

$$\frac{dE_s}{dz} = i\frac{\omega_s d_{eff}}{n_s c} E_o E_p^* \exp(i\Delta k \cdot z) \tag{2a}$$

$$\frac{dE_p}{dz} = i\frac{\omega_p d_{eff}}{n_p c} E_o E_s^* \exp(i\Delta k \cdot z) \tag{2b}$$

$$\frac{dE_o}{dz} = i\frac{\omega_o d_{eff}}{n_o c} E_s E_p \exp(i\Delta k \cdot z) \tag{2c}$$

where E_s, E_p, and E_o are the electric field strengths of the signal, pump and output light, respectively; n_s, n_p and n_o are the indices of refraction at the three wavelengths; d_{eff} is the effective nonlinear coefficient of the crystal; c is the speed of light, and z is the longitudinal position along the propagation direction of the output light within the crystal. Δk represents the phase mismatch, which is defined by:

$$\Delta k = \left| \vec{k}_o - \vec{k}_s - \vec{k}_p \right| \tag{3}$$

At perfect phase-matching condition, Δk equals zero.

Single-photon up-conversion devices use the principle of SFG to convert the single photon signal light to a wavelength that is efficiently detectable by single photon detectors such as a Si-APD. Because the signal light is at single photon levels and the pump power is much stronger than the signal ($E_p >> E_s$), the pump power intensity does not deplete significantly in the up-conversion process, resulting in the approximation $\frac{dE_p}{dz} \approx 0$. Therefore, Eq. 2(a-c) can be reduced to two coupled first-order differential equations.

There is no input at the sum wavelength ($E_{o(z=0)}=0$), which is the initial condition for the equations. By solving the equations with this initial condition, the probability of upconversion (or its transfer function response in general) is given as follows:

$$P_o(z) \approx \sin^2(\alpha\sqrt{I_p}z) \tag{4a}$$

where I_p is the intensity of pump light. α is the conversion coefficient of the non-linear media and can be estimated by the following equation:

$$\alpha \approx \left(\frac{\omega_s \omega_o d_{eff}^2}{n_s n_o c^2}\right)^{1/2} \tag{4b}$$

From Eq. 4 (a, b), one can see that the up-conversion efficiency is a sinusoidal oscillation with respect to pump power. There is an optimal pump power, at which the conversion efficiency reaches its maximum. For perfect phase-matching, the conversion efficiency can be as high as 100%.

According to Eq. 4 (a, b), in order to obtain high conversion efficiency, we need to increase the pump intensity while maintaining or even reducing the optimal pump power since stronger pump power can lead to more noise. Furthermore, it can be seen from Eq. 4 (a) that a longer interaction length, z, will increase the conversion efficiency. Choosing materials with high non-linear coefficients is another option for increasing the conversion efficiency.

2.2 Birefringent phase matching

From Eq. 1(a, b), we can write the phase matching conditions as:

$$\omega_s + \omega_p = \omega_o \tag{5a}$$

$$n_s\omega_s + n_p\omega_p = n_o\omega_o \tag{5b}$$

Because all non-linear crystals have dispersion, (i.e. the refractive index is wavelength dependent), it is impossible to satisfy the Eq. 5(a, b) simultaneously if the three light beams have the same polarization. In practice, we can use the birefringence of the crystal to satisfy the phase matching condition. A beam of light may be decomposed into two rays (the ordinary ray, or o-ray and the extraordinary ray, or e-ray) when it passes through a birefringent material. Many optical materials are birefringent, which means the refractive index depends on the polarization of the light beam. In that case, one can select beams with different polarization direction and align the crystal to satisfy the Eq. 5 (a, b) and thus implement phase matching. The main two types of birefringence phase matching are Type I (e.g. o-ray+o-ray→e-ray) and Type II (o-ray+e-ray→e-ray).

The advantage of birefringence phase matching is that it is perfect phase matching (Δk is zero). However, birefringence phase matching has several limitations, including:

1. Wavelength selection is limited by the materials birefringent refractive index and orientation angles. Therefore, not all wavelengths can find a suitable material and orientation angle to implement phase matching.
2. The most severe problem for birefringent phase-matching is walk-off in which the e-ray and the o-ray travel in different directions. This walk-off limits interaction length and reduces the internal conversion efficiency.
3. The nonlinear coefficients for the birefringent phase-matching conversion process are relatively low. For example, the largest coefficient for the birefringent phasematching in lithium niobate crystal is only -4.64 pm/V (d_{31}) [Dmitriev et al, 1999].

Due to these limitations, birefringent phase matching can not implement high efficiency frequency conversion, and is therefore not suitable for up-conversion detectors.

2.3 Quasi-phase-matching

To overcome the limitations associated with birefringent phase matching, a new approach has been developed. Having the pump beam, signal beam and output beam all be collinear and aligned to the same polarization orientation will overcome the problem of walk-off and will also take advantage of larger non-linear coefficients. Specifically, all beams are in the extraordinarily polarization mode, and therefore the highest nonlinear coefficient, d_{33} = -40 pm/V [Dmitriev et al, 1999], can be used, which is an order of magnitude higher than d_{31}. However, in that case, it is impossible to satisfy the perfect phase-matching condition shown in Eq. 5 (a, b), and therefore we need to use another scheme called quasi-phase-matching.

To explain the quasi-phase-matching technique, we must go back to Eq. 2 (a-c). If all light beams are collinear and have the same polarization orientation, birefringent phase-matching is not achieved and $\Delta k_Q \neq 0$. In this case, the "sign" of dE_o/dz is flipped when z changes by $\pi/\Delta k_Q$, resulting in the periodic cancellation of the electrical filed strength of the output beam E_o. By reversing the domain poles every $\pi/\Delta k_Q$, the quasi-phase-matching technology contributes an alternating "sign" component over the same period, ensuring that there is a positive energy flow from the signal and pump frequencies to the output frequencies, even

though all the frequencies involved are not phase locked with each other. The electrical field strength of the output beam versus the longitudinal position along the waveguide, with and without periodical poling, is shown in Fig. 2. Since the typical period for complete conversion to the output electrical field is on the order of thousands of poling periods, the evolution of the output field is well characterized by a sine function of the longitudinal position. Therefore, we can ignore the small fluctuations illustrated in Fig. 2 and approximate the full up-conversion process for the poled system with Eq. 4 (a, b)

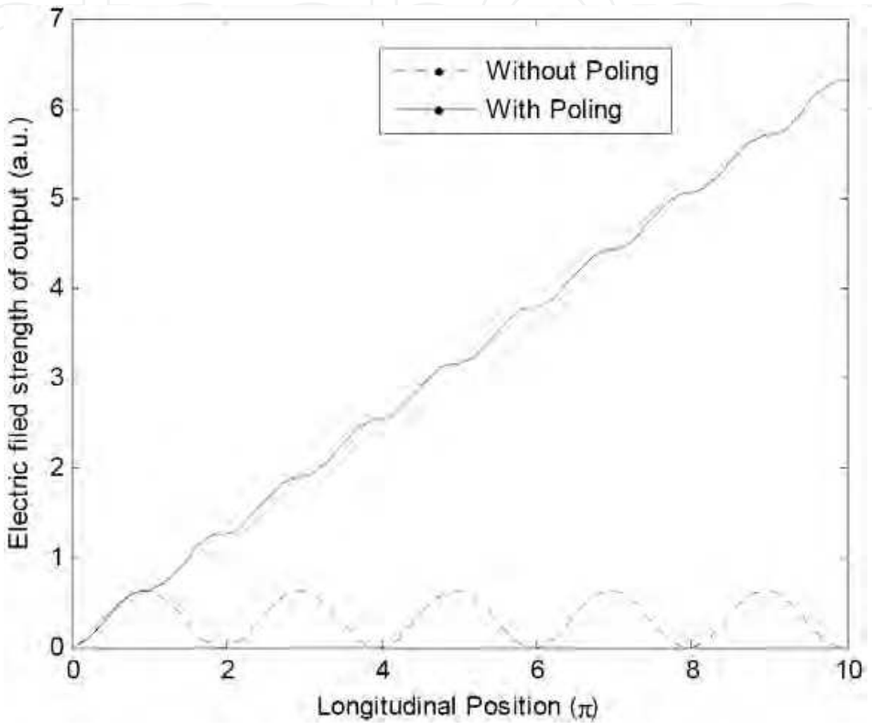

Fig. 2. Electric field strength of the output light versus the longitudinal position with poling and without periodic poling.

In terms of the phase, the periodic "sign" change results in an extra term ($2m\pi/\Lambda$) in Eq. 3. Λ is the poling period for the m^{th} order quasi-phase-matched condition of the nonlinear PPLN waveguide. Because all three beams are collinear, their wavevectors have the same direction and we are able to show the phase relation in one dimension in Fig. 3.

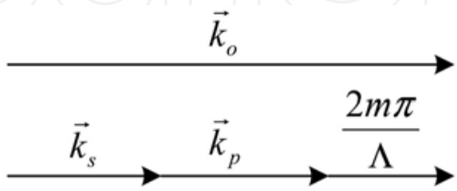

Fig. 3. Phase-match condition in quasi-phase-matching.

The phase mismatching is determined by the Eq. 6:

$$\Delta k \equiv k_o - k_s - k_p - \frac{2m\pi}{\Lambda} \tag{6}$$

where k_s ,k_p ,k_o are the wave numbers of the signal, pump and output beams in the crystal. By properly selecting Λ, the poling period of the crystal, the quasi-phase-matching is satisfied such that Δk =0. In the most desirable first-order (m=1) quasi-phase-matching condition, the ideal period can be calculated by using the following equation:

$$\Lambda = 2\pi/(k_o - k_s - k_p) \tag{7}$$

Once the ideal period, Λ, is calculated, a suitable mask can be designed with the ideal period imprinted and a photo-lithographic technique may then be used to make a periodic pattern on a nonlinear material substrate. When the substrate is heated and an intense electric field applied to the region exposed by the mask, the electrical field flips the direction of the nonlinear susceptibility of the crystal. After annealing, the periodically poled material is ready to use. Fine tuning of the Λ is achieved by adjusting the crystal temperature since the refractive index of the crystal is a function of temperature.

In quasi-phase-matching, the phase is not perfectly matched in each poling period but it ensures that positive energy is converted from the signal and pump frequencies to the output frequencies throughout the whole optical length of the crystal. Due to the imperfect phase matching in each poling period, the effective nonlinearity is reduced and can be estimated by the following equation:

$$d_{eff} = (\frac{2}{\pi})(\frac{1}{m})d_{33} \tag{8}$$

All even number orders (m=2, 4, 6…) of the quasi-phase-matching technique will have no output since periodical cancellation of the electrical filed strength of output light will occur. For all odd number orders (m=1, 3, 5…), according to Eq. 8, the first-order (m=1) quasiphase- matching has the highest effective nonlinear coefficient, though it is relatively hard to fabricate since the periods are shorter. Third-order (m=3) quasi-phase-matching, on the other hand, is often used as the longer periods are easier to fabricate. Because d_{33} is much larger than d_{31} in lithium niobate, the effective nonlinear coefficient in third order quasiphase matching is larger than that in birefringent phase matching.

Quasi-phase-matching can remove constraints on finding wavelengths and beam orientation angles to satisfy phase matching, and allow use of the highest nonlinear coefficient. The greatest advantage of the quasi-phase-matching technique is the elimination of walk-off and subsequently, the longer allowable interaction distance within the crystal. Furthermore, all three beams can be coupled together into a crystal waveguide, in which a higher beam intensity and longer interaction distance leads to significantly higher conversion efficiency.

As mentioned, the quasi-phase-matching in periodically poled lithium niobate allows us to take advantage of the larger d_{33} nonlinear coefficient. With a waveguide implementation of the PPLN, a higher intensity of pump can be provided and a longer interaction distance becomes possible. Currently, PPLN waveguides are the most suitable devices to implement frequency up-conversion with almost 100% internal conversion efficiency achievable with relatively low noise.

3. NIR Up-conversion detector

Recently, several highly efficient up-conversion single photon detectors for the NIR range have been demonstrated using PPLN waveguides [Xu et al., 2007; Diamanti et al., 2005;

Langrock et al., 2005; Thew et al., 2006; Tanzilli et al., 2005] and bulk PPLN crystals [Vandevender & Kwiat, 2004]. In this section, we will describe in detail an up-conversion detector developed at NIST [Xu et al., 2007] and analyze its characteristics.

3.1 NIST Up-conversion detector configuration

The NIST detector uses an up-conversion device to convert single photons at 1310 nm, with a pump at 1550 nm, to photons at 710 nm that are then efficiently detected by a Si-APD.

The configuration of the NIST up-conversion detector is shown in Fig. 4. A 1550 nm continuous wave (CW) laser provides the pump seed. If needed, the seed light can be modulated to an optical pulse train by a synchronized signal. This feature is similar to an optical gate, which is very useful for noise reduction or high speed gating operation in a communications system. The modulated 1550 nm pump seed is then amplified by an erbium-doped fiber amplifier (EDFA) (IPG: EAR-0.5K-C). Two 1310/1550 wavelength division multiplexer (WDM) couplers with a 25 dB extinction ratio are used to clean up the 1550 nm pulsed pump, specifically suppressing any EDFA noise that may extend to 1310 nm. The amplified 1550 nm pump light is then combined with a weak 1310 nm signal by another WDM coupler and the combined pump and signal are then coupled into the PPLN waveguides. The waveguide is a reverse-proton-exchange PPLN waveguide with magnesium oxide doping. The input polarization state of both the signal and the pump are adjusted by the polarization controllers, PC1 and PC2 respectively, to align with the polarization of a waveguide before entering the coupler. From Eq. 2, we know that a longer waveguide will require less pump power to reach the maximum conversion efficiency. The PPLN waveguide in the NIST up-conversion detector is 5 cm, the longest possible with current fabrication capability. The input of the PPLN waveguide is fiber coupled, while the output is free-space with a 710 nm anti-reflection (AR) coating to increase transmission of the converted output signal. The output light of the PPLN waveguide, including the newly generated photons at 710 nm (SFG), the pump at 1550 nm and its second harmonic generation at 775 nm, are separated by two dispersive prisms. The pump light (1550 nm) is clearly separated after the first prism and blocked by a beam block. Because the 775 nm beam is close to the 710 nm being detected, a second dispersive prism is used to further separate them, and an adjustable iris is used to block the 775 nm photons. Because all the light beams are linearly polarized and their polarization is aligned with the p-polarization direction of the prisms, there is no intrinsic loss when the incident angle of the 710 nm light is close to the Brewster's angle. A 20 nm band-pass filter (Omega Optical, Inc.: 3RD700-720) is used to reduce other noise, such as photons leaked into the system from any external sources. The 710 nm photons are then detected by a Si-APD (PerkinElmer: SPCM-AQR-14).

3.2 Detection efficiency

Detection efficiency is the one of the most important metrics in single photon detectors. The overall detection efficiency of an up-conversion detector is determined by the internal conversion efficiency in the PPLN waveguide, the coupling and component insertion losses, as well as the detection efficiency of the Si-APD at the converted wavelength. The overall detection efficiency of an up-conversion detector can be estimated by the following formula:

$$\eta_o = \eta_{loss} \cdot \eta_{con} \cdot \eta_{\det} \approx \eta_{loss} \cdot \eta_{\det} \cdot \sin^2(\alpha \cdot \sqrt{I_p} \cdot L) \tag{9}$$

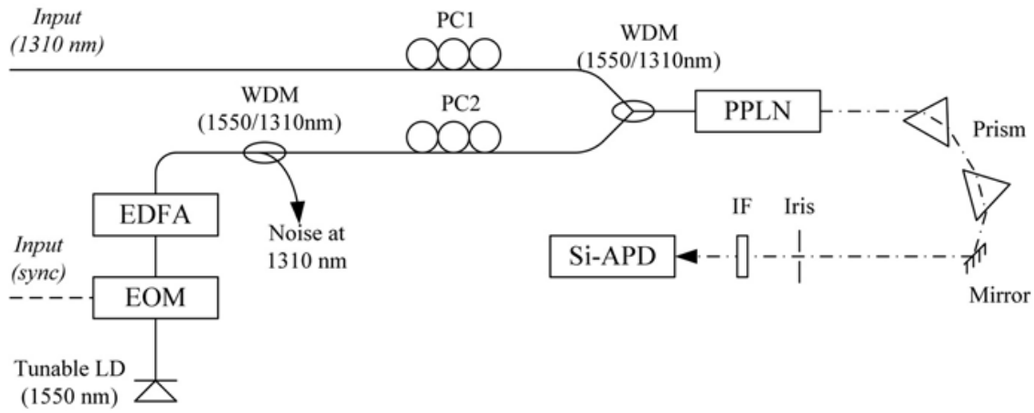

Fig. 4. Schematic diagram of the up-conversion detector. EOM: Electric-optic modulator; EDFA: Erbium-doped fiber amplifier; WDM: Wavelength-division multiplexing coupler; PC: Polarization controller; PPLN: Periodically-poled LiNbO3 waveguides; IF: Interference filter. Solid line: Optical fiber; Dash line: Free space optical transmission.

where η_o is the overall detection efficiency of the up-conversion detector; η_{loss} is the total loss in the detector, including the component insertion loss and waveguide coupling loss; η_{con} is the internal conversion efficiency in the PPLN, and can be estimated by Eq. 4; and $\eta_{\det}$ is the detection efficiency of the Si-APD at the converted wavelength, which at 710 nm is specified to be about 65 %.

When the insertion and coupling losses, the detection efficiency of the Si-APD and the structure of the waveguide are fixed, the overall conversion efficiency of the detector is determined by the internal conversion efficiency of the waveguide, which is dependent on the pump intensity with a $\sin^2(\sqrt{\ })$ relationship according to Eq. 9. The measured conversion efficiency versus pump power in a CW mode and in a pulsed pump mode is shown in Fig. 5. The measured results are in agreement with the estimated value from Eq. 9. The maximum detection efficiency is 32 % for both pump modes, which corresponds to 100 % internal conversion efficiency after excluding the insertion loss and the Si-APD detection efficiency.

In many quantum information systems, the photons arrive along with a classical signal that is synchronized to the photon transmission. That transmission clock can be recovered from the classical signal and used to operate the up-conversion detector in a pulse pump mode. The detection efficiency measured here is from a 625 MHz synchronized classical signal with 600 ps (FWHM) pulses. The quantum optical pulse is pumped with the same synchronized signal but has a shorter 300 ps (FWHM) pulse width. The detector operating in pulse pump mode can reach the maximum conversion efficiency with a lower average pump power, which helps to reduce the noise (discussed in detail in the next section). In cases where there is not a synchronized signal, a CW pump is needed. For pulse pump and CW pump modes, the optimal pump power (average) is about 38 mW and 78 mW, respectively.

3.3 Noise reduction

For a single photon detector, the noise level, or dark count rate, is the most important performance parameter since a higher dark count rate can cause more errors in the quantum information system and degrade the system's fidelity.

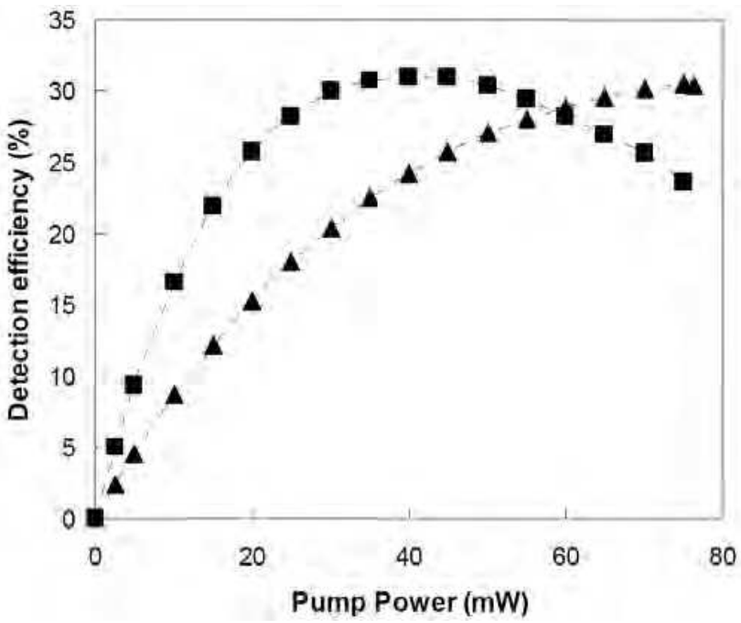

Fig. 5. The detection efficiency as a function of pump power. Two cases are shown: CW pump (triangle) and pulsed pump (square).

The dark count rate has been extensively studied in frequency up-conversion technology [Xu et al., 2007; Diamanti et al., 2005; Langrock et al., 2005; Thew et al., 2006]. The dark counts are contributed mainly by three parts: the intrinsic dark counts of the Si-APD, dark counts caused by the noise in the pump tail at the signal wavelength, and dark counts caused by the Raman scattering. The intrinsic dark count rate is constant, about 100 c/s in the NIST system. The dark counts caused by the noise in the pump tail occur as the pump noise at 1310 nm is up-converted to 710 nm and detected by Si-APD. About a 20 kHz dark count rate caused by the noise from the pump is observed at the maximum conversion efficiency. We use two WDM couplers (a 50 dB extinction ratio in total) to greatly suppress this noise. The dark counts caused by the Raman scattering occur as 1310 nm photons are generated by Raman scattering with the strong pump light in the transmission fiber and waveguide, and then up-converted to 710 nm and detected by Si-APD. In this up-conversion detector unit, we use a 1550 nm laser as a pump, whose wavelength is longer than that of the quantum signal we want to measure. Because the anti-Stokes component of the Raman process is much weaker than the Stokes component, a dark count rate of less than 2400 c/s is achieved when the conversion efficiency is maximized.

As shown in the Fig. 6, the pulse pump generates more dark counts than the CW pump for a given average power, because the peak power of the pulse pump is higher than the average power. However, the pulse pump needs less average power than the CW pump to achieve a given detection efficiency, see Fig. 5, and in the end, the pulse pump can achieve a given detection efficiency with less dark counts than the CW pump. As an example, the maximum detection efficiency is reached at 38 mW pulse pump resulting in a dark count rate of 2400

c/s. For the CW pump, on the other hand, a pump power of 78 mW is required to achieve the maximum detection efficiency, which incurs a dark count rate of 3100 c/s.

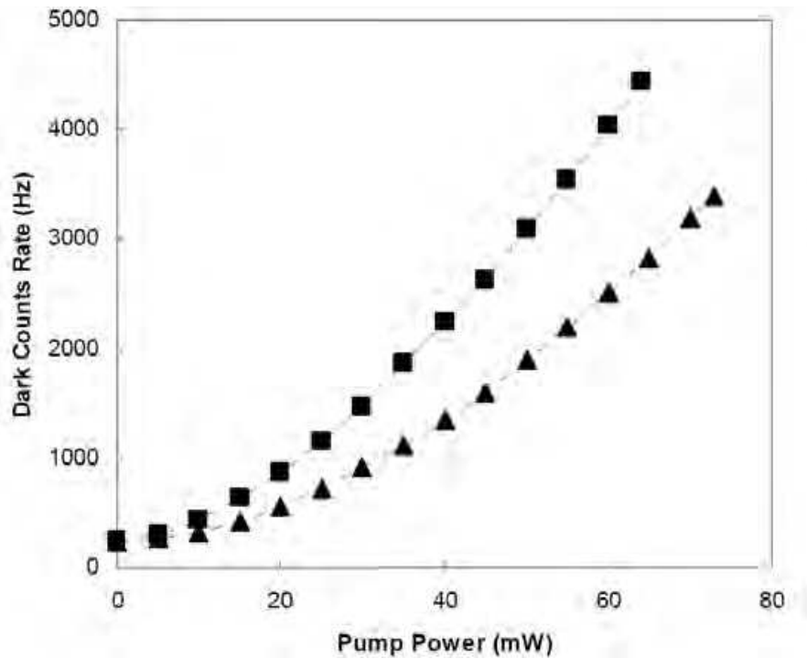

Fig. 6. The dark count rate as a function of pump power at the PPLN input. Two cases are studied: CW pump (triangle) and pulsed pump (square).

3.4 Wavelength and temperature response

When the quasi-phase matching condition in a PPLN waveguide is satisfied at a particular signal wavelength, the maximum up-conversion efficiency is achieved. When the signal is shifted from that wavelength the up-conversion efficiency is reduced. Therefore, the upconversion detectors have a narrow wavelength acceptance width, similar to a narrow band pass filter. While it helps to filter out noise at wavelengths other than the signal wavelength, this may be a drawback when the detector is used to measure photons with wider spectrums. The acceptance spectral width of the up-conversion detector is determined by the transfer function response of the PPLN waveguide. The transfer function response of a finite-length uniform QPM grating in the waveguide is a function of a $\mathrm{sinc}^2(\ )$ as follows [Fejer et al, 1992; Micheli 1997]:

$$P_o(\Delta k_Q) \propto P_p \cdot P_s \cdot \mathrm{sinc}^2(A \cdot \Delta k_Q \cdot L) \tag{10}$$

where P_o, P_p, P_s are the powers of SFG output, pump, and signal beam; A is a constant; L is the waveguide length; and Δk_Q is the phase-mismatch, which can be calculated by the following relation with the system wavelengths:

$$\Delta k_Q = 2\pi \cdot \left(\frac{n_o}{\lambda_o} - \frac{n_p}{\lambda_p} - \frac{n_s}{\lambda_s} - \frac{m}{\Lambda}\right) \tag{11}$$

where λ_o, λ_p and λ_s are the wavelengths for output, pump, and signal, respectively, and n_o n_p and n_s are the reflective index for the three wavelengths. Λ is, as described earlier, the poling period for the mth order quasi-phase-matched condition of the nonlinear PPLN waveguide. From Eq. 2 and 3, the acceptance spectral width is dependent on the length of the waveguide, the longer the waveguide, the narrower the acceptance spectral width will be. Fig. 7 shows the measured detection efficiency as a function of the signal wavelength at a fixed pump wavelength and temperature. From the figure, we can see that the spectrum is similar to the sinc^2( ) function and the acceptance spectral width of the main peak is about 0.25 nm (FWHM). If we use a short waveguide or a pump light with a wider spectrum, the acceptance spectral width can be broadened.

The up-conversion wavelength peak is also temperature sensitive. Therefore, one or both of the pump and signal wavelengths, or the waveguide temperature, must be accurately tuned to achieve the maximum up-conversion efficiency. To investigate the temperature sensitivity of the up-conversion, we sent a 1 mW CW 1310 nm laser beam with a linewidth of less than 10 MHz into the PPLN waveguide. Moreover, we turned off the pump seed laser so that the amplified spontaneous emission (ASE) noise from the EDFA acted as the pump. Using an optical spectrum analyzer, we measured the spectrum at the output of PPLN waveguide at different temperatures from 50 °C to 70 °C. The resulting output spectrum is shown in Fig. 8, normalized to the peak power after we subtracted the ASE spectrum.

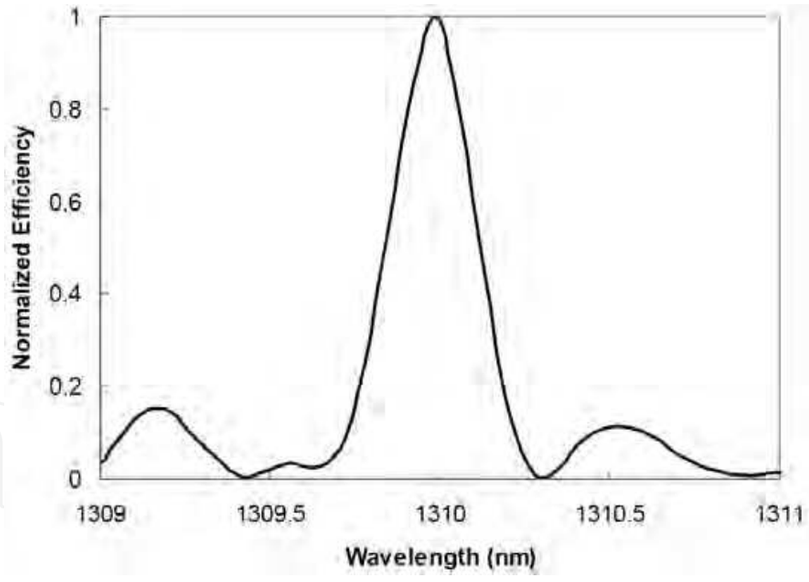

Fig. 7. The normalized detection efficiency as a function of signal wavelength, when the pump wavelength and temperature of the waveguide are fixed.

As shown in Fig. 8(a), the spectral width of the sum frequency at 710 nm is about 0.15 nm. The result is consistent with the spectral width of 0.25 nm for the signal at 1310 nm as shown in Fig. 7. Also from Fig. 8(a), the peak wavelength is shifted as the temperature changes, which means that the quasi-phase matching condition can be achieved by either varying the

converted wavelength (via tuning of the pump wavelength and/or signal wavelength), or by varying the waveguide temperature, as shown in Fig. 8 (b). Within a temperature variation range of 20 degrees, the central wavelength for maximum efficiency linearly varies by approximately 1.1 nm. The temperature response of the waveguide can provide a method to fine tune the up-conversion detector, even if the signal and pump wavelengths are fixed.

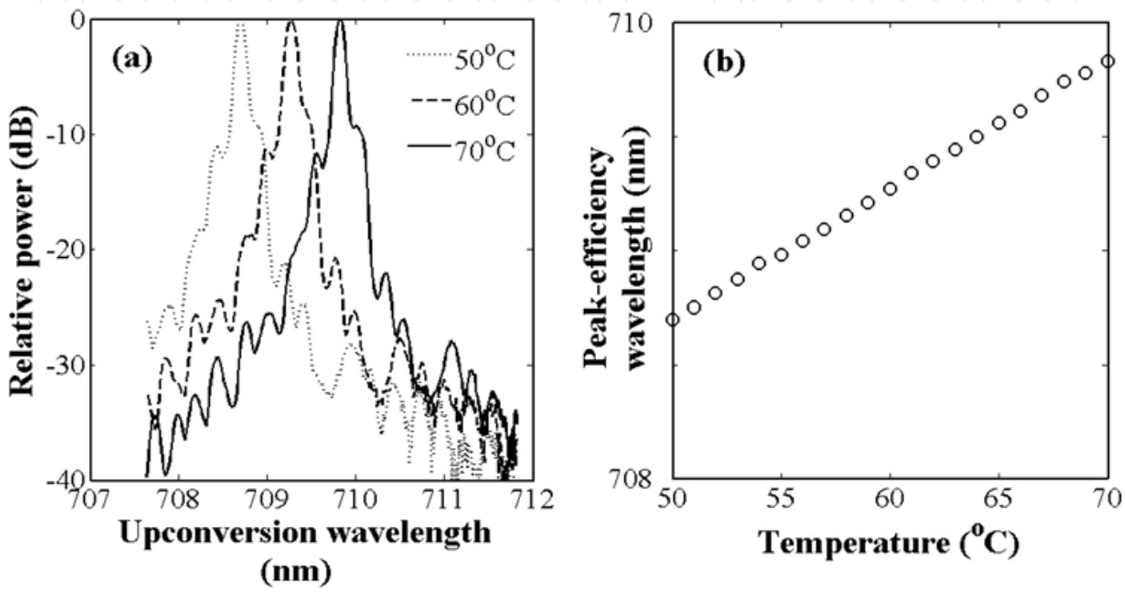

Fig. 8. (a) The normalized output spectrum of the PPLN at different temperatures. (b) The up-conversion wavelength peak as a function of temperature.

3.5 Polarization characteristic

Because the PPLN waveguide is based on proton-exchange, it is effective only for guiding the e-wave, and the o-polarized light is not transmitted. In effect, the device is therefore polarization sensitive. If its polarization extinction ratio is sufficiently high, the device can be used as a polarizer. This feature is very useful in a polarization-encoding quantum communications system. Fig. 9 shows the dependence of the detection efficiency on the polarization direction of an input signal at 1310 nm. The deviation angle is the angle (in Jones space) between the given input polarization state and the one at which the conversion efficiency is maximized. We also compared this measurement result with a $\cos^2(\ )$ curve, the function which represents an ideal polarizer. The curve is in good agreement with the measured data and we believe that the slight difference is caused by the measurement uncertainty of the polarimeter. As shown in Fig. 9, the polarization extinction ratio of the PPLN is over 25 dB. Therefore, an up-conversion detector can be used as a polarizer in a polarization-based quantum information system, eliminating the need for an otherwise required polarizer and avoiding the additional insertion loss that a polarizer would add.

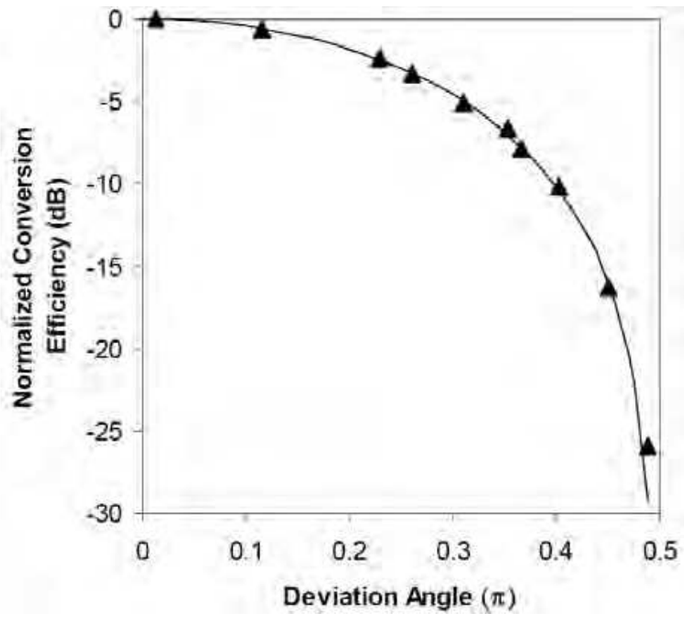

Fig. 9. The normalized conversion efficiency of the PPLN waveguide as a function of deviation angle of the input signal at 1310 nm. The deviation angle is the angle between the given polarization state and the state at which the conversion efficiency is maximized. Triangle: Measurement results; Solid line: $\cos^2()$ curve

4. Application in quantum communication systems

Quantum key distribution (QKD) is an important application of quantum communication, which is a technique for developing shared secret keys over unsecured communication channels that is guaranteed by the fundamental quantum properties of single photons instead of mathematical complexity [Gisin et al., 2002]. It is not possible to make a perfect copy (clone) of an unknown quantum state, thus precise measurement by an eavesdropper is not achievable. The Heisenberg uncertainty principle states that pairs of quantum properties cannot be precisely measured simultaneously; for example, position and momentum. Horizontal-vertical and diagonal polarization of photons is another such pair.

QKD systems use quantum states, such as polarization, to encode information on single photons. An initial random key is established by randomly encoding quantum state information on these photons, transmitting the photons and recovering the encoded state information at the other end of the link. After sifting, error correction and privacy amplification, the three conventional processing procedures required to complete the QKD protocol, the initial (raw) keys become secure keys and are ready for use.

The idea to use quantum states to securely encode information originated with Stephen Wiesner in 1983 [Wiesner, 1983]. This idea was taken forward by Charles Bennett and Gilles Brassard in 1984 [Bennett & Brassard, 1984] who developed the famous QKD protocol called BB84, which uses four quantum states. In 1992, Charles Bennett proposed a simplified version of the protocol, named B92, [Bennett, 1992] that uses only two quantum states. These

two protocols are commonly used in most QKD systems today. The first demonstration of a QKD system was completed in 1989, in which the quantum channel was a 30 cm long path of air in a laboratory [Bennett & Brassard, 1989]. Since then, a number of groups have successfully developed many experimental QKD systems, which are described in a comprehensive review article by Nicolas Gisin [Gisin et al., 2002].

Single photon detectors are one of the key elements for a QKD system since information is encoded as the quantum state of single photons. Among the available types of single photon detectors, up-conversion detectors are quite suitable for QKD systems due to their high detection efficiency, low dark count rate and unique characteristics, such as narrow acceptance spectral width and polarization sensitivity. Specifically, the advantages offered by up-conversion detectors include:

1. High detection efficiency: many QKD systems use a narrow linewidth attenuated laser light as the single photon source, which is much narrower than the acceptance bandwidth of up-conversion detection. Therefore, an up-conversion detector can reach its maximum detection efficiency, resulting in a higher secure key rate.
2. Low dark count rate: many QKD systems recover the clock signal from their classical channel, which can also be used as the synchronized trigger for the pulse pump operation in an up-conversion detector. As described earlier, the pulse pump operation of the up-conversion detector can lead to a lower dark count rate and, therefore, a lower system error rate.
3. Narrow acceptance spectral width: each up-conversion detector has a relatively narrow acceptance spectral width that functions as a band-pass filter, rejecting the noise due to crosstalk from strong signals in classical channel that share the same fiber in many QKD systems.
4. Polarization sensitivity: as described earlier, this feature can be used as a polarizer, which avoids the additional insertion loss that an otherwise required polarizer would add.

Because of these outstanding performance characteristics, several research groups have successfully demonstrated fiber-based QKD systems using up-conversion single photon detectors. By way of an example, we introduce a fiber-based QKD system developed at NIST[Xu et al., 2007]. The system uses the B92 protocol [Bennett, 1992] with 1310 nm photons that share a single optical fiber with bi-directional classical signals at the 1550 nm band.

A QKD system using the B92 protocol requires two detectors to detect the photons emerging from the two different measurement bases. Fig. 10 outlines a compact dual up-conversion detector system, and is an all fiber system rather than the free-space output configuration described in Fig. 3. A weak pump seed laser is amplified by an EDFA and split into two parts, each of which will provide the pump for one of the detectors. Each detector in this dual detector system consists of a 5 cm PPLN waveguide, whose input and output are fiber coupled. The detectors use in-line narrow band-pass filters to suppress noise from the pump light and its SHG component. This all fiber detector is easy to use and more compact compared to the free space output detector described earlier, however its overall detection efficiency is reduced to 15~20 %, due to output coupling loss from the waveguide to the fiber and the insertion loss associated with the narrow band-pass filters.

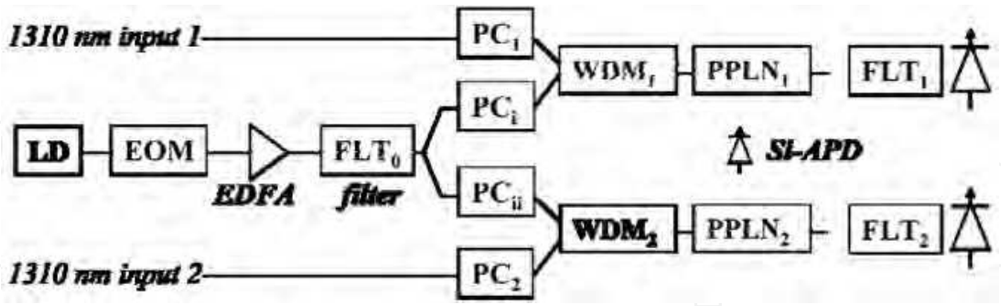

Fig. 10. The configuration of compact dual up-conversion detectors. LD: Laser diode; EOM: Electric-optic modulator; EDFA: Erbium-doped fiber amplifier; FLT: Optical filter; PC: Polarization controller; WDM: Wavelength-division multiplexer for 1310 nm and 1550 nm; PPLN: PPLN waveguide.

The configuration of the QKD system using the up-conversion detector is shown in the Fig. 11. The system is designed to generate a secure key between a sender (Alice) and a receiver (Bob). The QKD system uses a custom printed circuit board with a field-programmable gate array (FPGA) [Mink et al., 2006] to generate a random stream to encode the photon with quantum state information and to transmit and receive classical data. The classical data is carried by a conventional optical signal at 1550 nm.

To polarization-encode the quantum channel with the random data, we first modulate a 1310 nm CW beam into a 625 MHz pulse train which is evenly split into two polarization channels. Each pulse train is further modulated by one of two complementary 625 Mbit/s quantum channel data streams. The two quantum channels are then combined by a 45-degree polarization-maintaining combiner and attenuated to a mean photon number of 0.1 per bit, and then multiplexed with the classical channel before being coupled into a standard single-mode fiber for transmission.

At the receivers end, another WDM is used to demultiplex the quantum and the classical channels. A clock signal is recovered from classical channel and it is sent into the upconversion detectors as the synchronized trigger for the pulse pump operation. Photons in the quantum channel are randomly split into two non-orthogonal measurement bases by a coupler and are then sent to their respective up-conversion detectors. The up-conversion detector's polarizer-like characteristic performs a polarization measurement on the photons which are then converted and detected. For each detection event, the bit position, but not the bit value, of the detected photon is returned to Alice over the classical channel. Alice's FPGA matches each detection event with the corresponding event of the stored bit-stream. The matched positions, again without the bit values, are returned to Bob. Both Bob and Alice send the bit values to their respective CPUs for reconciliation and privacy amplification to generate their shared secret keys, which are then used in a conventional security application.

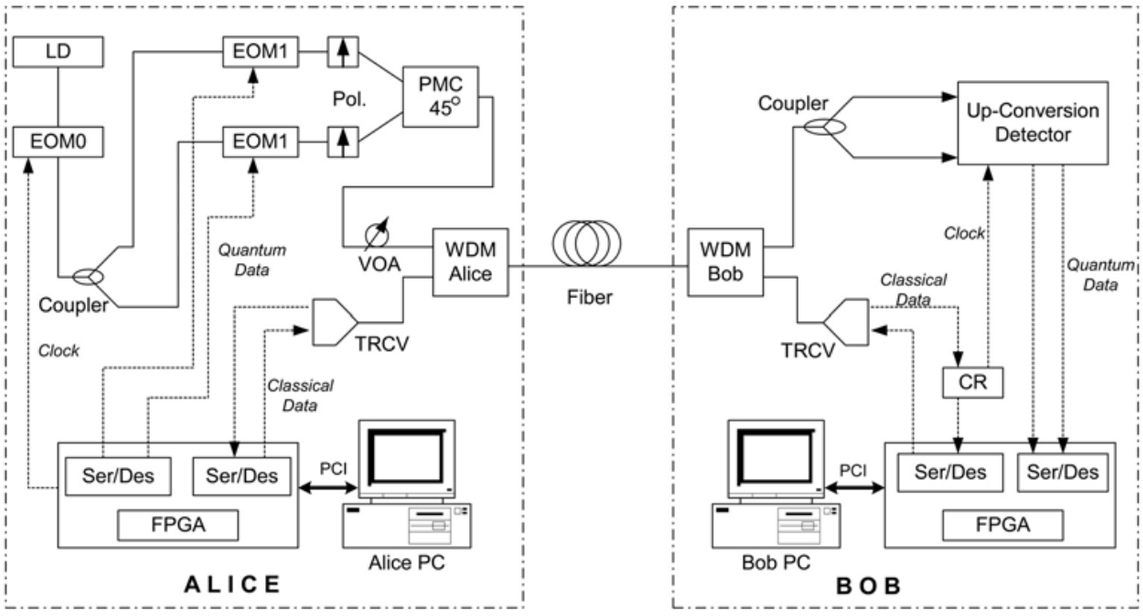

Fig. 11. The B92 polarization coding QKD system. LD: Laser diode; EOM: Electric-optic modulator (LiNbO3); PC: Polarization controller; PMC-45°: Polarization maintaining combiner that combines two light signals that are separated by 45 degrees; VOA: Variable optical attenuator; WDM: Wavelength-division multiplexer; SMF: Standard single-mode fiber; TRCV: Optical transceiver; CR: Clock recovery module; FPGA: Custom printed circuit board controlled by a field-programmable gate array; PCI: PCI connection; Up-conversion detector: See Fig. 8; Dotted line: Electric cable; Solid line: Optical fiber.

In theory, the security of a QKD system is guaranteed by the fundamental principles of physics and cannot be broken. However, in practice its security is limited by its noise level. The noise level, or dark count rate, is therefore the main concern for QKD system development and implementation. Although the up-conversion detector has a low darkcount rate, other sources of noise must be identified when the detector is integrated into a system. In the QKD system, the quantum channel (1310 nm) and the bi-directional classical channel (1510 nm & 1590 nm) share a single standard telecom fiber, so there is a concern that the quantum channel may suffer from noise from the classical channel. In a QKD system that uses up-conversion detectors, the crosstalk from the strong signal in the classical channel (1510 nm & 1590 nm) will be blocked by the narrow acceptance spectral width of the up-conversion detector. In the classical channel, there are two noise sources including a small amount of noise around 1310 nm emitted from the transceivers and noise due to nonlinear effects, which is widely believed to be from Raman scattering. This is similar to the 1550 nm pump noise in the up-conversion detector discussed in section 3.3. The strong signals at 1510 nm and 1590 nm interact with the fiber and, in a nonlinear anti-Stokes process, generate photons around 1310 nm. These 1310 nm fiber generated photons enter the PPLN waveguides and are up-converted to 710 nm. Fig. 12(a) shows the extra dark count rate induced by the classical channel at various fiber link distances. We first measure the

dark count rate when one or both of the classical transceivers are on, and then subtract the dark count rate measured when both transceivers are off. The photon leakage can be evaluated by the extra dark counts in a back-to-back (0 km) connection while the nonlinearly induced dark photon effect will vary over the transmission distance. As shown in the Fig. 12(a), the photon leakage noise is small and the dark counts are mainly induced by the Raman anti-Stokes process, particularly from the classical signals at 1510 nm propagating from Alice to Bob (forward anti-Stokes). The backward anti-Stokes noise is generated by the classical signals at 1590 nm propagating from Bob to Alice and is much weaker than the forward anti-Stokes because of the greater separation between the 1590 nm light and the nm signal photons. In general, the classical channel induces a non-negligible

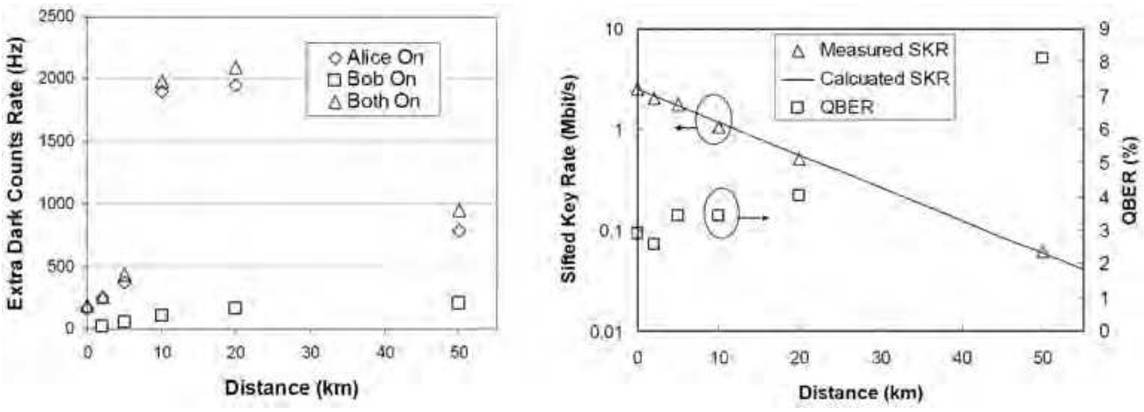

Fig. 12. (a) The extra dark count rate induced by the classical channel in one of the PPLN detector in three cases: Diamond, only the transceiver at Alice is on; square, only the transceiver at Bob is on; triangle, both transceivers are on. The other PPLN detector exhibits similar behaviors. (b) The system performance of the B92 polarization-based QKD system with the 1550 nm pumped up-conversion detector.

dark count rate into the QKD system, particularly from 1510 nm. A longer wavelength transceiver would greatly help to reduce the dark count rate further, but care must be taken to keep it within the standard telecom band.

The system performance is shown in Fig. 12(b). During our measurements, the pump power was fixed at 40 mW. The sifted-key rate is 2.5 Mbit/s for a back-to-back connection, 1 Mbit/s at 10 km, and 60 kbit/s at 50 km. The quantum bit error rate (QBER) is approximately 3 % for the back-to-back configuration, remains below 4 % up to 20 km, and reaches 8 % at 50 km. The finite extinction ratio of the modulator and timing jitter of the system induces a background QBER of approximately 2.5 % and the remaining QBER results from dark counts generated by both the pump light and the classical channel, as we described earlier. We also calculated the theoretical sifted-key rate and QBER and they agree with the measured results. Although we fixed the pump power close to the maximum up-conversion efficiency, the QBER remains small until 20 km due to the low dark count rate of the 1550 nm up-conversion detector. The QKD system can generate sufficient secure keys in real time for one-time-pad encryption of continuous 200 kbit/s encrypted video transmission over 10 km.

5. Conclusion

Frequency up-conversion single photon detectors use the principle of sum frequency generation to up-convert single photons in the near IR range to a shorter wavelength for an efficient detection by low cost detectors, such as Si-APDs. The up-conversion detectors are usually operated at room temperature with high detection efficiency and a low dark count rate. The detectors have a very narrow acceptance spectral width and polarization sensitivity, properties that can be exploited in certain applications requiring narrow linewidth or polarization specific detection. These unique characteristics can be used to enhance system performance in some applications, including fiber-based quantum communications systems.

6. References

Bennett, C. H. & Brassard, G. (1984). Quantum cryptography: Public key distribution and coin tossing. *Proc. IEEE Int. Conf. Comput. Syst. Signal Process*., pp. 175–179.

Bennett, C. H. & Brassard, G. (1989). The Dawn of a New Era in Quantum Cryptography: the Experimental Prototype is Working .*SIGACT NEWS,* Vol.20, pp. 78-83

Bennett, C. H. (1992). Quantum cryptography using any two nonorthogonal states. *Phys. Rev. Lett.*, Vol. 68, pp 3121-3124

Boyd, R. W. (2008). Nonlinear Optics, Academic Press, ISBN 978-0123694706, New York. Diamanti, E.; Takesue, H.; Honjo, T.; Inoue, K. & Yamamoto, Y. (2005). Performance of various quantum-key-distribution systems using 1.55-μm up-conversion singlephoton detectors. *Phys. Rev. A,* Vol. 72, 052311

Dmitriev, V.G.; Gurzadyan, G. G. & Nikogosyan, D. N. (1999) Handbook of Nonlinear Optical Crystals, Springer, ISBN 978-3540653943

Fejer, M.; Magel, G.; Jundt, D. & Byer, R. (1992). Quasi-phase-matched second harmonic generation: tuning and tolerances. IEEE J. Quantum Electron. Vol.28, pp 2631-2654

Gisin, N.; Ribordy, G.; Tittel, W. & Zbinden, H., (2002). Quantum cryptography. *Rev. Mod. Phys.* Vol. 74, pp 145–195

Goetzberger, A.; McDonald, B.; Haitz, R.H. & Scarlett, R.M. (1963). Avalanche effects in silicon p-n junctions. II. Strucrually perfect junctions. *J. Appl. Phys.* Vol 34: 1591-1600

Gol'tsman, G. N.; Okunev, O.; Chulkova G.; Lipatov, A.; Semenov, A.; Smirnov, K.; Voronov, B. & Dzardanov, A. (2001). Picosecond superconducting single-photon optical detector. *Appl. Phys. Lett.* Vol. 79, pp 705-707

Gurski, T. (1973). High-quantum-efficiency infrared up-conversion. *Appl. Phys. Lett.*, Vol. 23, pp 273-275.

Hadfield, R.; Schlafer, J.; Ma, L.; Mink, A.; Tang, X. & Nam, S. (2007). Quantum key distribution with high-speed superconducting single-photon detectors. *CLEO/QELS Technical Digest,* QML4,

Hamamatsu. (2005). Near infrared photomultiplier tube R5509-73 data sheet.

Kim, Y.; Kulik, S. & Shih, Y. (2001) Quantum teleportation of a polarization state with a complete bell state measurement. *Phys. Rev. Lett.* Vol. 86, pp 1370-1373

Korneev, A.; Kouminov, P.; Matvienko, V.; Chulkova, G.; Smirnov, K.; Voronov, B.; Gol'tsman, G. N.; Currie, M.; Lo, W.; Wilsher, K.; Zhang, J.; Słysz, W.; Pearlman, A.; Verevkin, A. & Sobolewski, R. (2004). Sensitivity and gigahertz counting performance of NbN superconducting single-photon detectors. *Appl. Phys. Lett.* Vol. 84, pp 5338-5340

Langrock, C.; Diamanti, E.; Roussev, R. V.; Yamamoto, Y.; Fejer, M. M. & Takesue, H. (2005). Highly efficient single-photon detection at communication wavelengths by use of upconversion in reverse-proton-exchanged periodically poled LiNbO3 waveguides. *Opt. Lett. Vol.* 30, pp. 1725-1727

Lacaita, A.; Zappa, F.; Cova, S. & Lovati, P. (1996) Single-photon detection beyond 1 μm: performance of commercially available InGaAs/InP detectors. *Appl. Opt.,* Vol. 35, pp 2986-2996

Lita, A. E.; Miller, A. J. & Nam, S. W. (2008). Counting near-infrared single-photons with 95% efficiency," *Opt. Express,* Vol. 16, pp3032-3040

Ma, L.; Nam, S.; Xu, H.; Baek, B.; Chang, T.; Slattery, O.; Mink, A. & Tang, X. (2009). 1310 nm differential phase shift QKD system using superconducting single photon detectors. *New Journal of Physics,* Vol. 11, pp 054020

Martin, J. & Hink P. (2003) Single-Photon Detection with MicroChannel Plate Based Photo Multiplier Tubes. *Workshop on Single-Photon: Detectors, Applications and Measurement Methods, NIST*.

Micheli, M. P. (1997) χ^2 effects in waveguides. *Quantum Semiclassic. Opt*, Vol. 9, pp 155–164.

Midwinter, J. & Warner, J. (1967). Up-conversion of near infrared to visible radiation in lithium-meta-niobate. J. Appl. Phys. Vol 38, pp 519-523

Mink, A.; Tang, X.; Ma, L.; Nakassis, T.; Hershman, B.; Bienfang, J. C.; Su, D.; Boisvert, R.; Clark, C. W. & Williams, C. J. (2006). High speed quantum key distribution system supports one-time pad encryption of real-time video. *Proc. of SPIE,* Vol. 6244, 62440M,

Nakassis, A., Bienfang, J. & Williams, C. (2004). Expeditious reconciliation for practical quantum key distribution. *Proc. of SPIE,* Vol. 5436, pp. 28-35.

Takesue, H.; Nam, S.; Zhang, Q.; Hadfield, R. H.; Honjo, T.; Tamaki, K. & Yamamoto, Y. (2007). Quantum key distribution over a 40-dB channel loss using superconducting single-photon detectors. *Nature Photonics*, Vol. 1, pp 343-348

Tang, X.; Ma, L.; Mink, A.; Nakassis, A.; Xu, H.; Hershman, B.; Bienfang, J.; Su, D.; Boisvert, R.; Clark, C. & C. Williams. (2006). Experimental study of high speed polarizationcoding quantum key distribution with sifted-key rates over Mbit/s. *Optics Express*, Vol. 14, No.6, pp 2062-2070

Tanzilli, S.; Tittel, W.; Halder, M.; Alibart, O.; Baldi, P.; Gisin, N. & Zbinden, H. (2005). A photonic quantum information interface. *Nature,* Vol 437, pp 116-120

Thew, R. T.; Tanzilli, S.;, Krainer, L.; Zeller, S. C.; Rochas, A.; Rech, I.; Cova, S.; Zbinden, H. & Gisin, N. (2006). Low jitter up-conversion detectors for telecom wavelength GHz QKD. *New J. Phys.* Vol. 8, pp 32.

Vandevender, A. P. & Kwiat, P. G. (2004). High efficiency single photon detection via frequency up-conversion. *J. Mod. Opt.,* Vol. 51, 1433-1445

Wiesner, S. (1983). Conjugate coding. *Sigact News,* Vol. 15, pp 78-88

Wiza, J. (1979). Microchannel plate detectors. *Nuclear Instruments and Methods* Vol. 162: pp 587-601

Xu, H.; Ma, L.; Mink, A.; Hershman, B. & Tang, X. (2007). 1310-nm quantum key distribution system with up-conversion pump wavelength at 1550 nm. *Optics Express*, Vol 15, No.12, pp 7247- 7260

Yuan, Z. L.; Dixon, A. R.; Dynes, J. F.; Sharpe, A. W. & Shields, A. J. (2008). Gigahertz quantum key distribution with InGaAs avalanche photodiodes. *Appl. Phys. Lett.* Vol. 92, 201104.

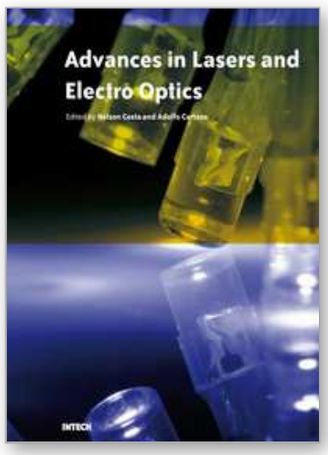

Advances in Lasers and Electro Optics

Edited by Nelson Costa and Adolfo Cartaxo

ISBN 978-953-307-088-9
Hard cover, 838 pages
Publisher InTech
Published online 01, April, 2010
Published in print edition April, 2010

Lasers and electro-optics is a field of research leading to constant breakthroughs. Indeed, tremendous advances have occurred in optical components and systems since the invention of laser in the late 50s, with applications in almost every imaginable field of science including control, astronomy, medicine, communications, measurements, etc. If we focus on lasers, for example, we find applications in quite different areas. We find lasers, for instance, in industry, emitting power level of several tens of kilowatts for welding and cutting; in medical applications, emitting power levels from few milliwatt to tens of Watt for various types of surgeries; and in optical fibre telecommunication systems, emitting power levels of the order of one milliwatt. This book is divided in four sections. The book presents several physical effects and properties of materials used in lasers and electro-optics in the first chapter and, in the three remaining chapters, applications of lasers and electro-optics in three different areas are presented.

InTech Europe
University Campus STeP Ri
Slavka Krautzeka 83/A
51000 Rijeka, Croatia
Phone: +385 (51) 770 447
Fax: +385 (51) 686 166
www.intechopen.com

InTech China
Unit 405, Office Block, Hotel Equatorial Shanghai
No.65, Yan An Road (West), Shanghai, 200040, China
中国上海市延安西路65号上海国际贵都大饭店办公楼405单元
Phone: +86-21-62489820
Fax: +86-21-62489821

IntechOpen